Microstructure analysis using temperature-induced contrast variation in small-angle scattering

John D. Barnes,[a]* Rainer Kolb,[b] Kathleen Barnes,[c] Alan I. Nakatani[c] and Boualem Hammouda[d]

[a]NIST Polymer Characterization Group, Gaithersburg, MD USA, [b]Exxon Research and Engineering, Annandale, NJ, [c]NIST Polymer Blends Group, Gaithersburg, MD, [d]NIST Center for Neutron Research, Gaithersburg, MD. E-mail: john.barnes@nist.gov

We propose to introduce Temperature-Induced Contrast Variation (TICV) as a technique for improving the specificity of microstructure analyses obtained using small-angle scattering methods. TICV exploits the fact that, at temperatures well removed from melting or annealing regimes, the scattering contrast in many multicomponent systems exhibits a significant temperature dependence while the form factors for the scattering processes change only slightly. Difference scattering patterns formed by subtracting the pattern measured at a suitable reference temperature from the pattern obtained at another temperature emphasize those components of the microstructure that vary most strongly with temperature over the chosen range. This can facilitate an effective separation of the observed scattering patterns into separate components for differing scattering mechanisms. Examples of distinct scattering mechanisms commonly found in polymers include liquid-like scattering from amorphous components, contributions from the intramolecular amorphous halo, Guinier scattering from inclusions, and the scattering from ordered stacks of crystalline lamellae.
The experimental data presented here provide qualitative demonstrations of general features of the method. Further work is needed to obtain improved descriptors to characterize microstructure in these systems.

1. Introduction

The work described below seeks to exploit the fact that, under certain favorable conditions, the intensity of the small-angle scattering (SAS) from certain polymeric materials varies strongly with temperature even though no microstructural changes are taking place. These effects are quite dramatic in semicrystalline polymers near their glass temperature. Figure 1 shows an example of this effect from recently published work (Barnes *et al.*, 1997).

Most, if not all, of the intensity variation in these cases arises from changes in the contrast factors that control SAS, namely the differences in scattering length density between the crystalline and amorphous elements in the microstructure. At the glass temperature, T_g, there is a sharp change in the thermal expansion coefficient of the amorphous component, which leads to a discontinuity in the temperature derivative of the scattered intensity.

Fischer *et al.* (1969) recognized the existence of this effect more than thirty years ago and sought to exploit it to help characterize glass transition effects in semicrystalline polymers that had previously proved to be elusive. The paper being presented here seeks to demonstrate, in a qualitative manner, that the temperature induced contrast variation (TICV) effect offers significant prospects for improving the characterization of morphology in semicrystalline polymers by a modest extension of the SAS methods that are currently in use.

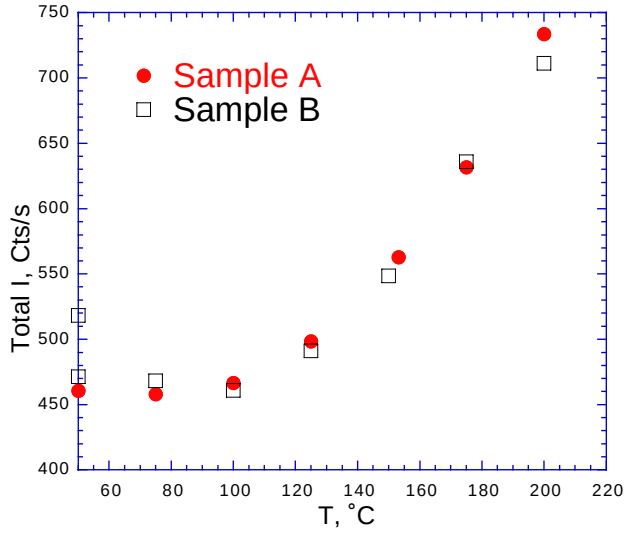

Figure 1
Integrated intensity as a function of temperature for two sPS samples from the work of Barnes *et al.* (1997).

2. Theory

The method of temperature-induced contrast variation makes extensive use of difference scattering patterns. Define $I\left(\overline{Q},T\right)$ as the intensity scattered into an element of solid angle at wavevector $q = 4\pi\frac{\sin\theta}{\lambda}$ and a temperature T. We take explicit account of any anisotropy that may be present in the structure by treating the wavevector as a three-dimensional entity. As will be shown later, anisotropy is extremely useful for confirming the identities of microstructural features.

A difference scattering pattern is defined by:

$$\Delta\left(\overline{Q},T\right) = I\left(\overline{Q},T\right) - I\left(\overline{Q},T_{ref}\right) = \frac{d}{dT}\left(I\left(\overline{Q},T\right)\right)\Big|_{T_{ref}}\left(T - T_{ref}\right) \quad (1)$$

where T_{ref} is a suitably chosen "reference temperature" and the derivative term represents a Taylor series expansion of the scattering law for the material under study.

Since modern SAS patterns are recorded digitally it is easy to take differences between patterns recorded under different conditions.

The contributions that vary most strongly with temperature dominate the right hand side of Eqn 1. Contributions to the full scattering pattern that are only weakly temperature dependent largely cancel out in the subtraction. Such contributions include incoherent backgrounds, solvent scattering, and some matrix effects in two-phase systems. It is normally quite difficult to account for these effects when analyzing full patterns, so that the difference method may offer considerably enhanced resolution in a number of instances.

The power of difference scattering has been demonstrated in the context of anomalous scattering (Haubold *et al.*, 1996) or with isotopic substitution in SANS (Higgins & Benoit, 1994). There is a very rich literature on the effects of temperature as the driving force for morphological change (including annealing, melting, phase separation, etc). Literature in which temperature is used to induce contrast variation while avoiding morphological change remains very scarce.

Setting aside for a moment the question of intensity scaling, it is common to treat the scattered intensity from two-phase systems

as the product of a contrast factor and a form factor (Glatter & Kratky, 1982; Feigin & Svergun, 1987).

$$I\left(\overline{Q},T\right) = \left(\Delta\rho\left(T\right)\right)^2 F\left(\overline{Q},T\right) \quad (2)$$

where $\left(\Delta\rho\left(T\right)\right)^2$ represents the contrast factor and $F(\overline{Q},T)$ accounts for the internal structure of the scattering moieties. In the present work we stipulate that the temperatures being employed are outside the range of temperatures at which gross morphological changes such as melting, annealing, or domain reorientation take place. If this requirement of morphological stability is met then changes in the form factor, $F(\overline{Q},T)$, can be neglected when interpreting the data.

3. Application: Lamellar Microstructures in Semicrystalline Polymers

As a first example of the power of the temperature-induced contrast variation method we consider the scattering from semicrystalline polymers well below their melting points. Our efforts to understand just such a system triggered our initial interest in these matters (see Figure 1). In this instance the dominant microstructural entities are stacks of lamellae organized into spherulites. The observed scattering contrast is attributable to the difference between the scattering length densities in the alternating amorphous and crystalline layers within these stacks. To first order in temperature we can express the scattering length density as:

$$\rho\left(T\right) = \rho\left(T_{ref}\right)\left(1-\alpha\left(T_{ref}\right)\left(T-T_{ref}\right)\right) \quad (3)$$

The contrast factor can then be expressed as:

$$\left(\Delta\rho\left(T\right)\right)^2 = \phi\left(1-\phi\right)\left(\rho_c\left(T\right)-\rho_a\left(T\right)\right)^2 = \phi\left(1-\phi\right)\left(\left[\rho_c-\rho_a\right]+\left[\rho_a\alpha_a-\rho_c\alpha_c\right]\left(T-T_{ref}\right)\right)^2 \quad (4)$$

where ϕ is the volume fraction crystallinity, the subscripts a and c label the amorphous and crystalline phases respectively, ρ is the scattering length density, and α is the volume coefficient of thermal expansion.

Defining a few simple parameters and combining Eqns 1, 3, and 4 leads to:

$$\Delta\left(\overline{Q},T\right) = 2\phi\left(1-\phi\right)\beta\delta T\left(\varepsilon+\beta\delta T\right)F\left(\overline{Q},T\right) \quad (5)$$

where $\delta T = (T - T_{ref})$, $\varepsilon = (\rho_c - \rho_a)$, and $\beta = (\rho_a\alpha_a - \rho_c\alpha_c)$. Note that the density and thermal expansion coefficient values to be used are those at the reference temperature. If T_g falls within the working temperature range one must be careful to take proper account of the discontinuity in the value of α for the amorphous component across T_g.

Equation 5 predicts that the amplitude of the difference pattern increases as a simple polynomial function of δT without any noticeable shifts in the peaks and valleys of the pattern. The relative strengths of the linear and quadratic terms in the polynomial are controlled by the differences between the bulk densities and the thermal expansions of the crystalline and amorphous phases. As long as there is no morphological change taking place the difference patterns should be reversible with respect to temperature.

Temperature-induced contrast variation is quite a striking effect. With proper precautions the technique yields difference scattering patterns that allow the observer to focus on specific features in the microstructure.

The most significant simplification in Eqns 2 through 5 is that the scattering is controlled by a single mechanism. In cases involving more than a single scattering mechanism it might be feasible to account for this by treating I(Q,T) in Eqn 2 as a mixture of components, each with its own contrast factor and geometric form factor.

In the remainder of this paper we will use Eqn 5 to interpret data from experiments on several different semicrystalline polymers. Generalizations of the method to other classes of materials are outside the scope of the present research.

4. Case I - Syndiotactic Polystyrene

Figures 1 and 2 are from previously published work (Barnes *et al.*, 1997) that piqued our interest in the TICV phenomenon. López *et al.* (1995) have examined the morphology of very similar samples. The formalism described in the preceding section accounts for the observed features as follows:

1. The sharp change in slope for the total detector count (Figure 1) in the vicinity of 100 °C corresponds to the glass transition in this polymer. This value is consistent with values estimated by other means (Pasztor *et al.*, 1991).

1a. The thermal expansion coefficients as well as the densities of the crystalline and amorphous phases differ only slightly below $T_g(\beta \approx 0)$. This accounts for the very weak temperature variation in the integrated $I(q)$ over the range 50 °C$\leq T \leq$100 °C.

1b. The thermal expansion coefficient of the amorphous phase increases dramatically at $T_g(\beta \gg 0$ for $T > T_g)$. This accounts for the strong temperature dependence for $T > T_g$ in Figure 1.

2. The absence of shifts in the peak positions for the circularly averaged difference patterns (See Fig 2) obtained between T_g and 200 °C is evidence for the stability of the lamellar stack microstructure.

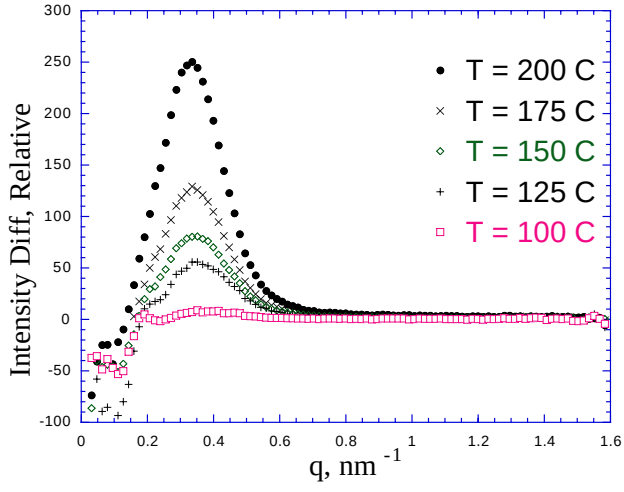

Figure 2
1-d difference SAXS patterns for sPS as a function of temperature. These patterns are obtained by circularly averaging 2-d difference SAXS patterns similar to those shown in Figures 3-5.

3. The relatively small negative values found at small q in Figure 2 reflect small decreases in the amplitude of the central scattering peak that occur when the sample is heated. We suspect that these represent annealing of structures on distance scales larger than the lamellar stacks (e. g. spherulites or voids). Such shifts seem to be commonplace in TICV experiments, but further work is required to elucidate their origin.

4. The intensities in Figure 1 are raw count totals over the entire detector. They therefore include contributions from the unscattered primary beam as well as a "matrix scattering" scattering that is distinct from the lamellar scattering. This matrix scattering is the major contributor to the baseline intensity (the values below 100 °C) in Figure 1. The origin of this scattering remains elusive.

5. Case II - poly(4-methyl pentene-1)(P4MP)

Poly(4-methyl pentene-1) is another polymer whose amorphous and crystalline densities are known to be very similar at temperatures below the glass temperature of the polymer (Griffith & Ranby, 1960; Lopez *et al.*, 1992; Litt, 1963). We obtained SAXS patterns from a small oriented sample. The orientation was produced by subjecting small pieces cut from a compression molded disk to plane strain compression using a channel die (Galeski *et al.*, 1992) at a temperature near the crystallization temperature. We find that orientation texture aids microstructural identification because each feature of the scattering pattern is seen in its proper geometrical relationship to other features.

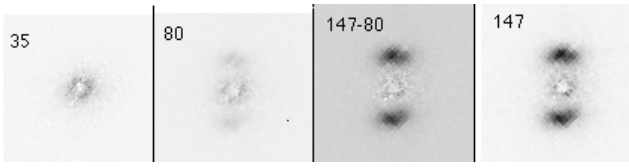

Figure 3
SAXS patterns for P4MP at 35 °C, 80 °C, and 147 °C. The difference between the 147 °C and 80 °C patterns is also shown.

Figure 3 shows portions of the P4MP scattering patterns obtained at temperatures of 35 °C, 80 °C, and 147 °C, together with the difference between the 147 °C and the 80 °C patterns. The melting temperature of this material is above 200 °C. The twin lobes that are prominent in the 147 °C pattern are the signature of scattering from oriented lamellar stacks. This feature is essentially absent at 35°C'because of the absence of contrast between the amorphous and crystalline components of this polymer below its T_g(ca. 60 °C). The lobes become more visible as the temperature increases above T_g. The literature is ambiguous with respect to the value of T_g for P4MP (Lopez *et al.*, 1992). Our TICV results support a value near 60 °C.

This strong correlation with the known behavior of the density of P4MP is very strong evidence for the appropriateness of the simple model set forth in Eqn 5.

In these patterns the scattering at low q is very weak. The 35 °C pattern in Figure 3 consists entirely of matrix scattering. This stands in sharp contrast to the data from sPS (Barnes *et al.*, 1997), so that it is reasonable to conjecture that the molecular architecture of the polymer has a strong effect on the matrix scattering. Other factors such as processing conditions, the existence of voids or other inclusions, etc. should also be considered when interpreting the low q scattering.

The low q scattering in the difference pattern of Figure 3 is very weak. There is no evidence of the annealing effects that contribute to the negative values in the 1-d difference patterns of Figure 2. This effectively confirms the argument of (Schultz, 1976) that much of the scattering observed at the lowest scattering angles in semicrystalline polymers should be attributed to causes other than the lamellar microstructure.

6. Case III SANS from Fluorinated Ethylene/propylene Copolymer

We decided to see how well the TICV method would work when used with neutrons. Our first test material was a commercial copolymer of tetrafluoroethylene and hexafluoropropylene. The material was supplied to as a strip approximately 50 mm wide. This material absorbs x-rays very strongly but it is highly transparent to neutrons. Since it composed entirely of carbon and fluorine its scattering is approximately 95 percent coherent.

Figure 4 shows the SANS patterns at 5 different temperatures together with the difference SANS patterns using the 25 °C pattern as a reference. The raw SANS patterns occupy the first and third rows of the array. The reference pattern is shown at the left end of the second row. The difference patterns are labelled with the two temperatures used in the difference. The melting point of this material is well above 200 °C

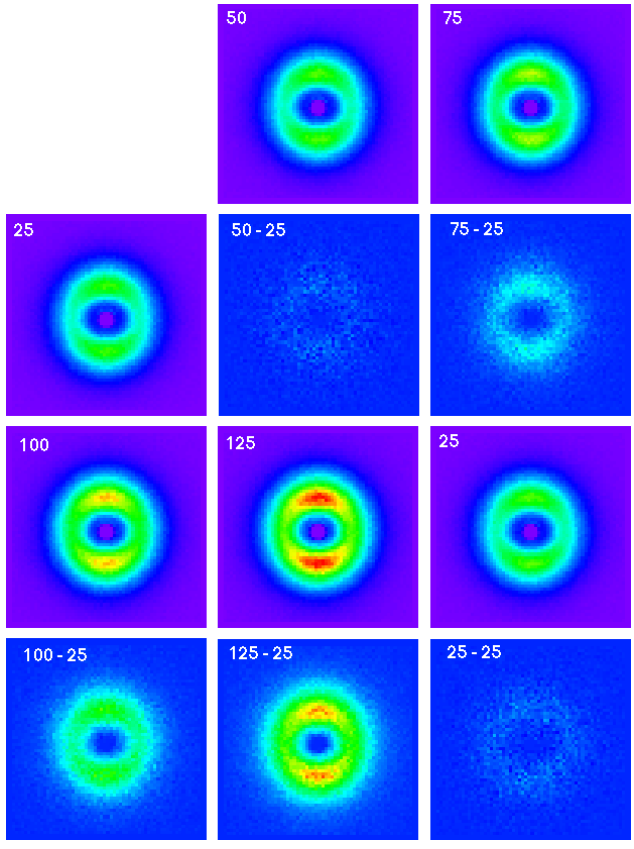

Figure 4
Raw SANS Data and difference SANS patterns for FEP copolymer. See text for explanation.

The very intense ring exhibiting a strong azimuthal peak is a classic example of scattering from the lamellar microstructure in a semicrystalline polymer. The direction of the azimuthal maximum coincides with the extrusion direction of the material.

The next notable feature of the raw SANS patterns in Figure 4 is the absence of scattering at very low q. This is quite rare in our experience. It will be interesting to compare SAXS and SANS patterns for this material because non-zero SAXS patterns would, in this case, be unambiguously assignable to voids. The lamellar SANS pattern for this material is not as strongly oriented as the others, presumably because the extrusion process that produced the material was relatively gentle.

The small residual lamellar scattering signal in the (25 25) difference pattern reflects the fact that the specimen had not actually cooled to 25 °C at the time the pattern was collected. Temperature cycling in this material did not introduce any low q scattering features of the kind seen in Figure 2.

There is no suggestion of a break in the intensity vs temperature curve for this material, which suggests that T_g for the FEP material is well outside of the range that we have studied. It is likely that T_g for this material is well below room temperature.

7. Case IV Polychlorotrifluoroethylene

The final example that we wish to present here is another SANS study, this time using a specimen of polychlorotrifluorethylene that we prepared by compression molding followed by extrusion in a channel die (Galeski *et al.*, 1992).

The SANS patterns in Figure 5 are arranged as in Figure 4, but in this case we observe strong scattering near the beam stop, with a streak extending perpendicular to the extrusion direction (which is horizontal in these images).

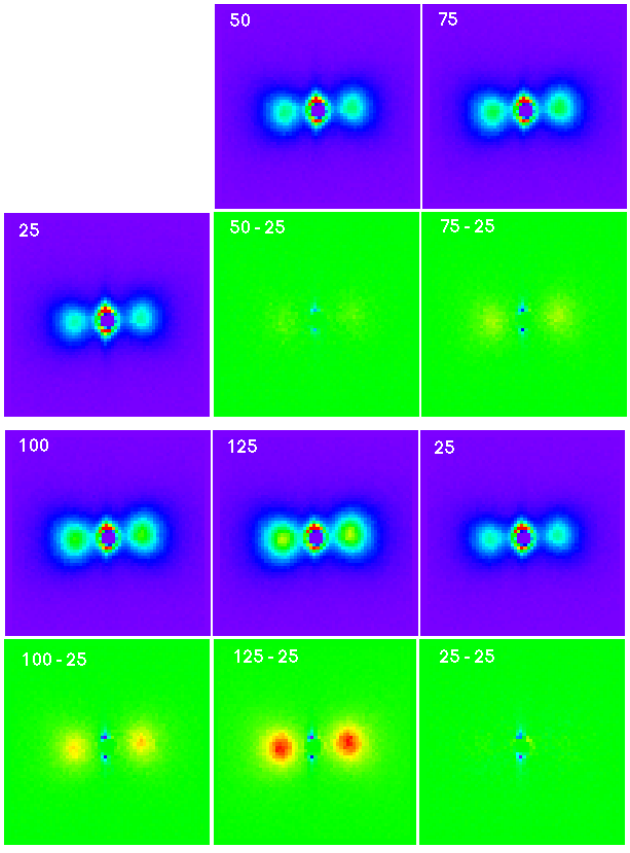

Figure 5
Raw SANS Data and difference SANS patterns for FEP copolymer. See text for explanation.

The component of the microstructure that gives rise to the central scattering and its associated streak remains to be identified. Strong streaks are often associated with fibrillar microstructures. Further complementary experiments using SAXS may help to sort out the issues.

The difference SANS patterns from the TICV experiments provide a dramatic demonstration that the scattering in the vicinity of the beam stop is associated with a contrast mechanism that is totally distinct from the one that gives rise to the lamellar microstructure. The central scattering is essentially absent in the difference patterns. The intensity of the two large lobes in the difference pattern increases strongly with temperature, indicating clearly that this feature arises from the lamellar microstructure.

The 25-25 difference pattern observed after heating the sample and cooling it back to room temperature exhibits two tiny negative-going peaks in the immediate vicinity of the beam stop. Since these features become increasingly negative as the sample traverses the temperature cycle, and since they in place after the sample is cooled back to room temperature, we must attribute them to a mechanism other than the lamellar scattering. This behavior is analogous to that observed for sPS.

8. Conclusions

The four examples of data obtained using the TICV method that we have presented are meant to illustrate the qualitative features of the results that can be expected when using this procedure. A number of improvements are needed before these data can be interpreted quantitatively. We felt, however, that the story told by the results shown here should be sufficient to motivate others to use this approach for their own work.

The data for the four example polymers is visually quite clean, with a high degree of morphological specificity.

The two-lobed structure that is the dominant feature of the difference SAS patterns for P4MP and PCTFE may well represent a suitable "basis function" for parameterizing SAS patterns from oriented lamellar stack microstructures. This feature conforms to our intuition regarding the proper form factor for the scattering from lamellar stacks in that we expect the strong scattering to be concentrated along the director for the stack and we expect it to be localized because of the periodicity in the stack structure.

The minimum in the scattered intensity near q=0 in the lamellar scattering function is not too surprising because the quasi-regular spacing in the lamellar stack morphology effectively builds a "correlation hole" into the form factor. Additional modeling work is need to substantiate this interpretation.

The difference patterns presented above clearly indicate that the low q component of the total scattering commonly observed from polymers is, in at least some instances, distinct from the lamellar scattering. This may well simplify the characterization of the lamellar microstructure by eliminating the artificial requirement for a Guinier term that is commonly employed in correlation function analyses (Strobl & Schneider, 1980). The suitability of SAS difference patterns for studying the limiting power law behavior has not yet been investigated.

In the cases of FEP and sPS (Barnes *et al.*, 1997) the observed pattern is the convolution of the dual lobe feature with a broad orientation texture distribution so that the lobes appear as arcs. To the extent that the arcs are not circular it is clear that the stack morphology depends on orientation. The relationship between orientation texture and stack morphology is a long standing issue in polymer science, but the TICV method may offer improved prospects for untangling the factors by providing cleaner input data.

We have consistently claimed that most, if not all, of the low q scattering seen in our studies must be attributed to something other than the lamellar stack morphology. Our data suggest that even the mild thermal treatments used here cause some annealing of the micrsotructural elements that are responsible for the low q scattering. Further work is need to understand these annealing effects. Since much of this scattering takes place behind the beam stop USAXS and light scattering studies are needed to better chracterize this feature of the scattering.

Protocols for conducting TICV measurements should probably be amended to require that the reference scattering patterns be obtained from well-annealed samples.

Detailed characterization of lamellar microstructures is often carried out using correlation function analyses (Strobl & Schneider, 1980). Our observations suggest that TICV difference patterns may provide better inputs to correlation function analyses because the difference patterns are relatively free of interfering effects. It should be noted that most correlation function analyses are carried out on samples that presumable scatter isotropically. We need to construct algorithms that are suitable for cylindrically symmetric systems in order to analyze the data obatined from our polymers.

The TICV method must be applied to a wider variety of semicrystalline polymers in order to characterize its sensitivity. A wider range

of microstructural types including block copolymers and amorphous polymers should be subjected to the method in order to determine whether it is useful for characterizing other aspects of polymer microstructure.

References

Barnes, J. D., McKenna, G. B., Landes, B. G., Bubeck, R. A. & Bank, D. (1997). *Polym. Eng. Sci*, **37**, 1480–1485.

Feigin, L. & Svergun, D. (1987). *Structure Analysis by Small-Angle Scattering of X-Rays and Neutrons*. Plenum Press, New York.

Fischer, E. W., Kloos, F. & Lieser, G. (1969). *Polymer Letters*, **7**, 845–850.

Galeski, A., Bartczak, Z., Argon, A. S. & Cohen, R. E. (1992). *Macromolecules*, **25**, 5705–5718.

Glatter, O. & Kratky, O. (1982). *Small-Angle Scattering*. Wiley, New York.

Griffith, J. H. & Ranby, J. (1960). *J. Polymer Sci.* **44**, 369–.

Haubold, H.-G., Wang, X. H., Jungbluth, H., Goerigk, G. & Schilling, W. (1996). *Journal of Molecular Structure*, **383**, 283–289.

Higgins, J. & Benoit, H. (1994). *Neutron Scattering in Polymers*. Clarendon Press, Oxford.

Litt, M. (1963). *J. Polymer Sci, Pt A*, **1**, 2219–2224.

López, L. C., Cieslinski, R. C., Putzig, C. L. & Wesson, R. D. (1995). *Polymer*, **36**, 2331–2341.

Lopez, L. C., Wilkes, G. L., Stricklen, P. M. & White, S. A. (1992). *J. Macromol Sci C, Revs in Macromolecular Chemistry and Physics*, **32**, 301–406.

Pasztor, A. J., Landes, B. G. & Karjala, P. J. (1991). *Thermochimica Acta*, **177**, 187–195.

Schultz, J. M. (1976). *J. Polym Sci., Polym Phys Ed*, **14**, 2291–2311.

Strobl, G. R. & Schneider, M. (1980). *J. Polym. Sci, Polym. Phys. Ed.* **18**, 1343–1359.